

The Measurement of Subcritical Electroconvection

I. Rehberg,¹ F. Horner,¹ and G. Hartung¹

Under idealized conditions, electroconvection in a nematic liquid crystal sets in at a well-defined threshold of the driving ac voltage. Fluctuating convection rolls of a small amplitude below that threshold have been observed recently. The measurement of the amplitude of these fluctuations is described in detail in this paper. It is based on averaging the light intensity signals using the structure function and a quantitative analysis of the light deflection.

KEY WORDS: Convection; electrohydrodynamics; fluctuations; shadowgraph; noise; structure function.

Electroconvection in a nematic liquid crystal has become a popular system for studies of pattern formation in nonequilibrium systems because of the easy control of the external parameters and the smallness of the cells, which lead to convenient time scales of the pattern formation processes (see ref. 1 for review). The smallness offers another advantage mentioned by Graham⁽²⁾: It should be possible to observe the macroscopic response of the system to thermodynamic fluctuations, namely fluctuating convection patterns below the onset of convection, resulting in a rounding of the bifurcation. Fluctuating convection patterns of very small amplitude below the onset of convection have indeed been observed recently.⁽³⁾ In this paper we describe in detail the procedure to measure the amplitude of these fluctuations which has been used in ref. 3, which contains averaging in space and time using the structure function and a quantitative analysis of the light deflection inside the cell.

The experimental setup used in ref. 3 is similar to that described in ref. 1. A layer of thickness $d = 13 \mu\text{m}$ of the nematic liquid crystal MBBA [*N*-(*p*-methoxybenzylidene)-*p*-butylaniline] is used. A preferred direction of the rolls above onset is enforced by rubbing of the glass slides which confine the sample. The temperature is controlled to ∓ 0.01 K. The

¹ Physikalisches Institut, Universität Bayreuth, D-8580 Bayreuth, Germany.

frequency of the applied voltage is 45 Hz. The voltage amplitude is the control parameter, and can be changed in 0.0035-V steps. The convective threshold was found to be $V_c = 7.142$ V. The shadowgraph intensity $I(x, t)$ is digitized at various times t and at 512 positions x along a line parallel to the wave vector of the convection rolls over a length of $14d$ (the entire sample is much larger than this).

Electroconvection in a nematic liquid crystal leads to a spatially periodic distortion of the director field. This field creates a periodically varying index of refraction $n(x, y, y')$ for the light polarized parallel to the director, given by

$$n(x, y, y') = n_o n_e [n_o^2 \cos^2(\beta) + n_e^2 \sin^2(\beta)]^{-1/2}$$

where β measures the angle between the light beam and the director as described in ref. 4, although due to a typographical error $n(x, y, y')$ is given incorrectly in ref. 4. The resulting path of the light beam has been understood quantitatively using Fermat's principle.⁽⁴⁾ The main result of ref. 4 for small director distortions is summarized in Fig. 1: The displacement Δy of the light, which is proportional to the intensity modulation measured on top of the cell, is proportional to the amplitude of the director distortion Θ . The angle of the outgoing light α is proportional to Θ^2 , and thus of small influence for the measurement of the very small angles Θ observed here. The value for the maximal displacement Δy has been calculated to be

$$\frac{\Delta y}{d} = 2\Theta \frac{\hat{n}}{1 + \hat{n}\pi}$$

with $\hat{n} = 1 - (n_e/n_o)^2$.

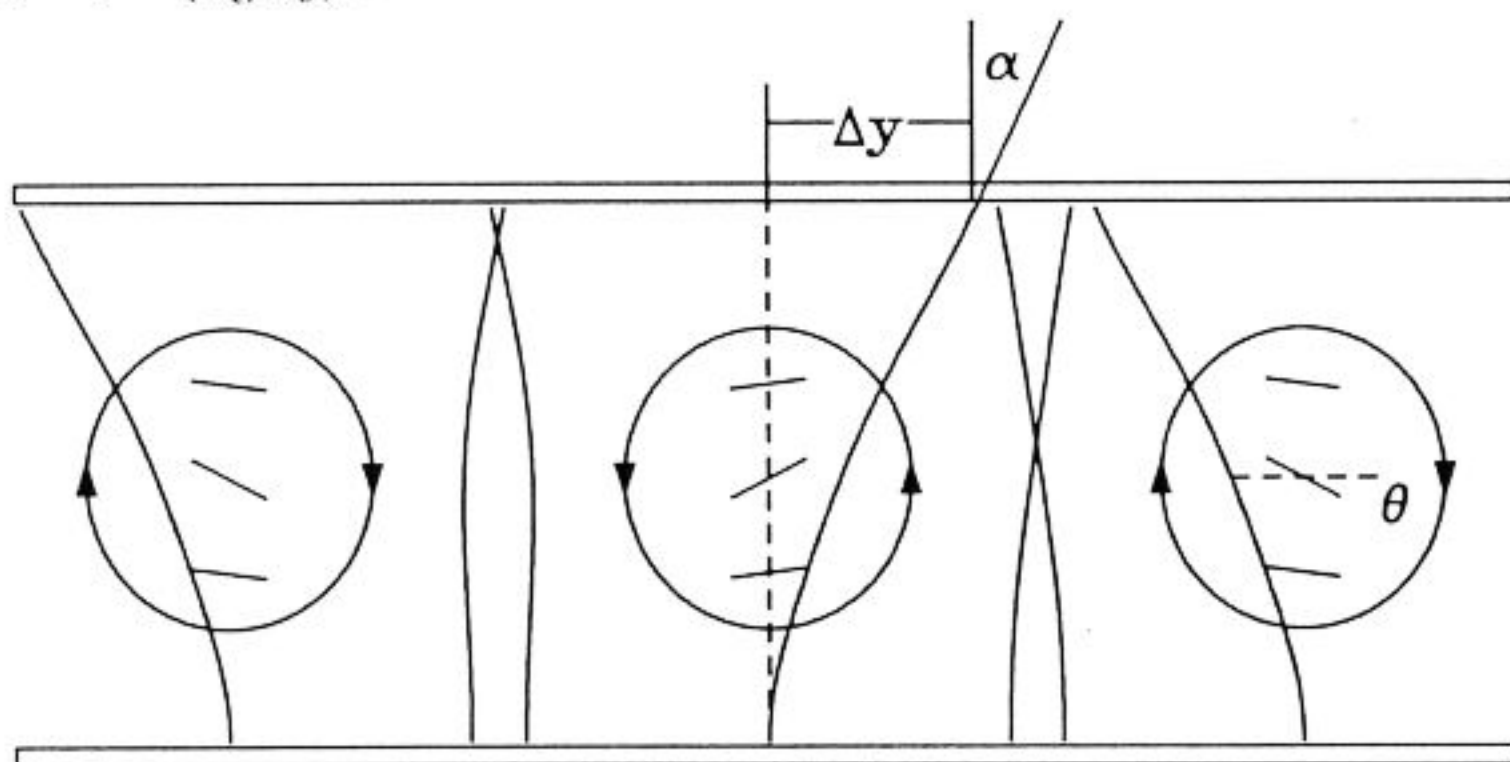


Fig. 1. The path of light polarized in the plane of the director. The motion of the fluid is indicated by the circles. The lines inside the circles indicate the director field. The light path has been calculated for a large director angle $\Theta = \pi/4$ rad for clarity and is indicated by the curves. The maximal displacement Δy of a light beam is proportional to Θ , and the maximal deflection angle α is proportional to Θ^2 for small Θ .

Using Eq. (7a) of ref. 4, this leads to a light intensity variation of

$$\begin{aligned}\frac{\Delta I}{I} &\approx 2\Theta \frac{\hat{n}}{1 + \hat{n} \pi} \frac{1}{kd} \\ &= 4\Theta \frac{\hat{n}}{1 + \hat{n} \lambda} d\end{aligned}$$

where λ is the wavelength of the convection pattern. Using the values of $n_e = 1.75$ and $n_o = 1.54$ (MBBA parameters), one gets

$$\Theta \approx (\Delta I/I)(\lambda/d) \cdot 0.61 \quad (1)$$

This relationship is valid for small angles Θ and independent of the height where the intensity profile is measured. This is very important for measurements because the distance f between the top of the cell and the focal plane of the microscope is usually hard to determine. The range of validity of (1), on the other hand, is sensitive to this distance f , as indicated by Fig. 2. Here the intensity calculated for a director angle $\Theta = 0.1$ rad at various distances f from the top of the cell is plotted. At a height of $f = 2d$ above the cell the tendency to form the strong (at the position of the upgoing flow) and the weak (at the position of the downgoing flow) real focus is clearly seen. At the top of the cell ($f = 0$) the intensity profile contains weaker higher harmonics. Below this point, higher harmonics with a different phase show up again, indicating the tendency to form virtual foci.

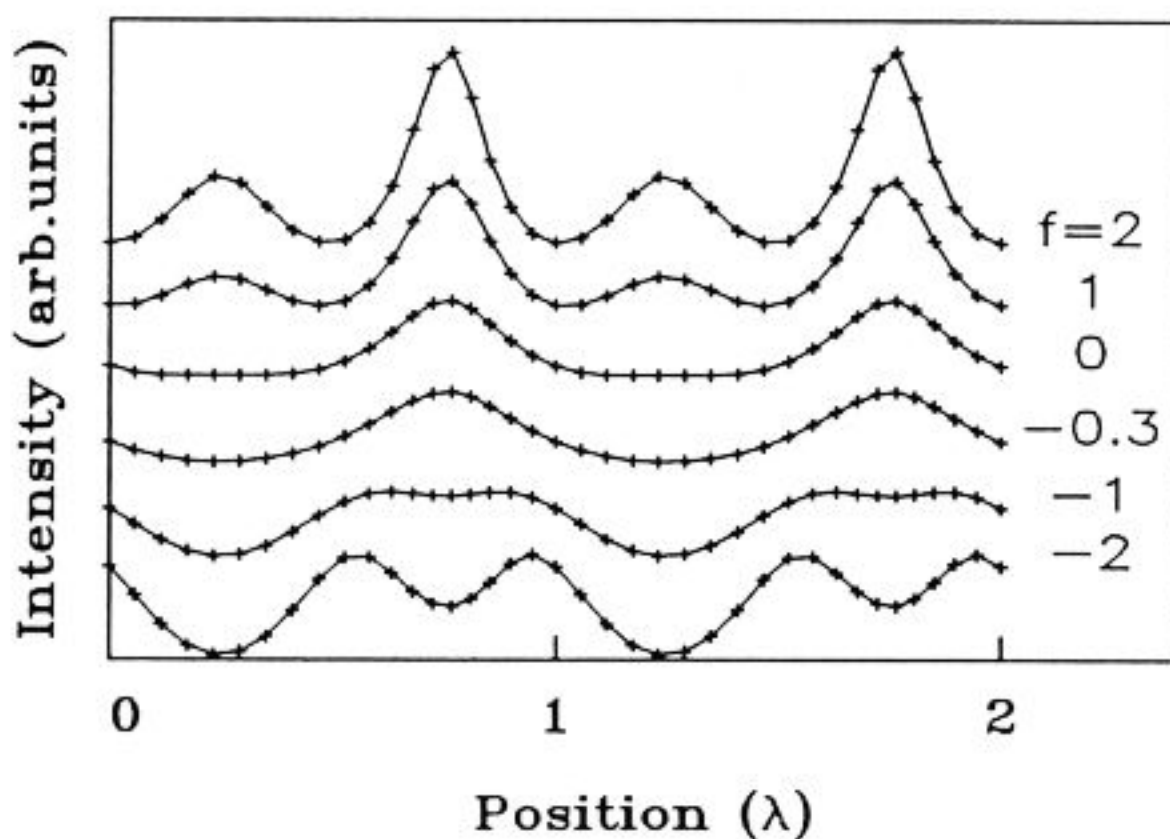


Fig. 2. The calculated intensity of an intensity profile perpendicular to the rolls, for a director angle of $\Theta = 0.1$ rad and a wavelength of $\lambda = 1d$. The labels indicate the distance between the top of the cell and the focal plane in units of the cell thickness d .

We have studied the range of validity of approximation (1) by comparing it with the results obtained by a numerical integration of the Euler-Lagrange equation describing the path of the light inside the cell.⁽⁴⁾ The result is presented in Fig. 3. The solid line represents Eq. (1). The open circles are the intensity modulation as measured by the root mean square of the light intensity variation. Experimentally, this is the most convenient procedure to measure the director angle Θ , but it has the disadvantage of being sensitive to the noise of the measuring system as well. An increase of the signal-to-noise ratio can be obtained by Fourier analysis of the measured intensity. The fundamental with the wavelength of the pattern grows proportional to Θ and is in reasonable agreement with the approximation (1) for values of Θ smaller than 0.1 rad. The higher harmonics come in at higher orders of Θ and were too small to be detected in the measurements presented in ref. 3, where one deals with angles $\Theta < 0.01$ rad.

As can be seen in Fig. 3, the range of validity of Eq. (3) is largest when focusing the microscope to the plane with the distance of $f = -0.3d$ from

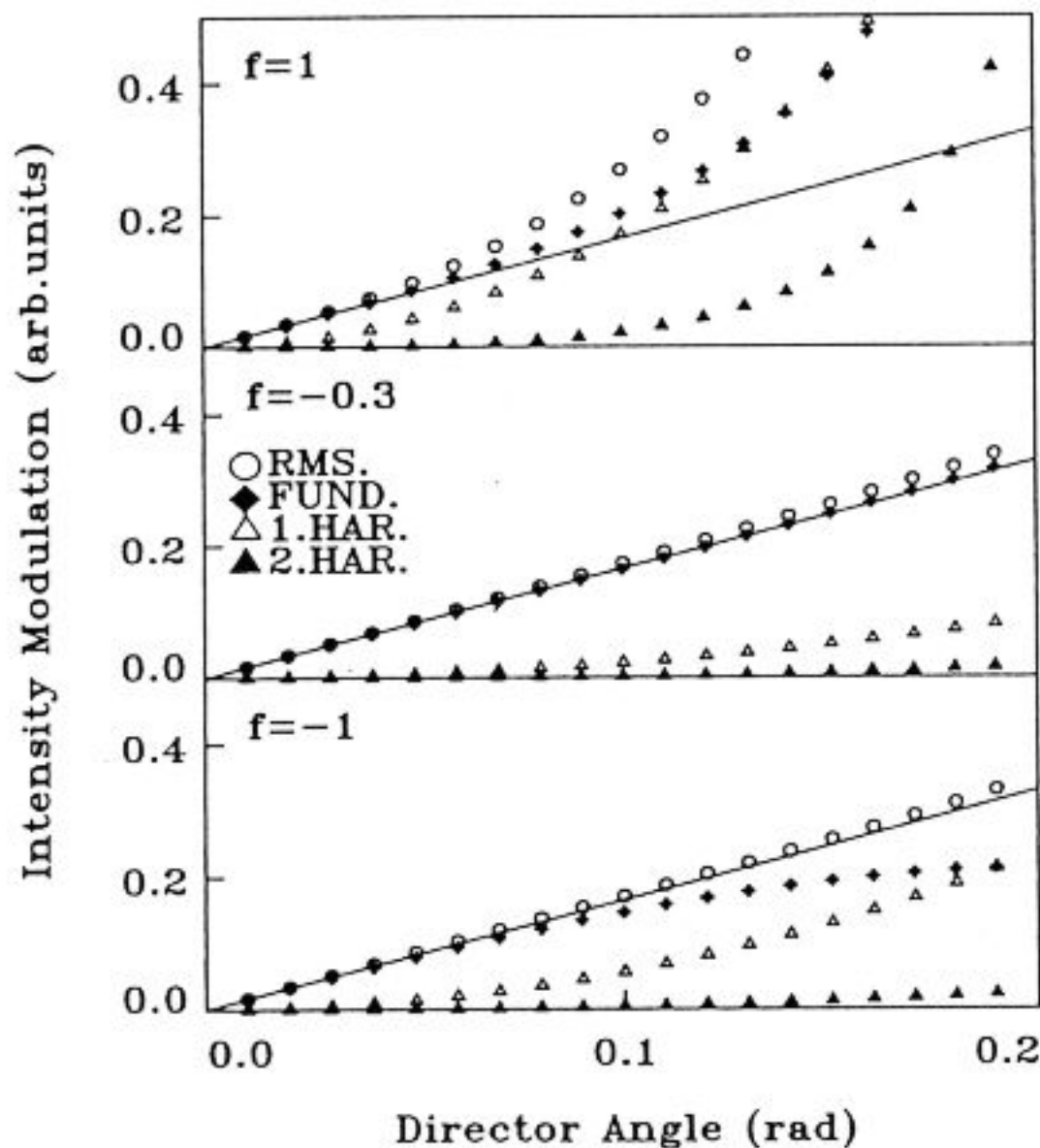


Fig. 3. The results of a spatial Fourier analysis of light intensity profiles similar to the ones shown in Fig. 2 are plotted as a function of the director angle for three different focal distances as indicated by the labels and a wavelength of $\lambda = 1d$. Open squares represent the rms value of a profile; solid diamonds the fundamental; open triangles, the first harmonic; and solid triangles, the second harmonic. The solid line represents the approximation of Eq. (1).

the top of the cell, i.e., close to the middle of the cell. This position can be found most conveniently by using a supercritical driving voltage. Then the position of the real and imaginary foci of the images can be located, and the middle between these two positions is a good approximation for the middle of the cell. Again, we like to stress the point that an exact knowledge of the distance is not needed, because approximation (1) is valid for any distance.

Another feature of the small-amplitude measurements presented here is the fact that the signal-to-noise ratio is smaller than 1 when measuring the intensity with our CCD-Camera and digitizer along a single line perpendicular to the rolls. The way to increase this ratio is by averaging many lines. In principle this could be done in Fourier space. In that case, however, the principal errors of a discrete Fourier transform like leakage would not be averaged out, and moreover the subtraction of the experimental background noise is complicated. Thus it is preferable to work in real space by adding spatiotemporal correlation functions. Because of the higher calculation speed and faster convergence, the correlation is obtained by using the structure function algorithm,⁽⁵⁾ i.e., one computes

$$S(\Delta x, \Delta t) = \sum_{x_i} \sum_{t_i} [I(x_i, t_i) - I(x_i + \Delta x, t_i + \Delta t)]^2$$

where x_i ranges from 0 to 255, while t_i ranges from 0 to 2047. The measured intensity varies between 0 and 255 due to the 8-bit digitizer. Thus the squares do not need to be calculated, but can be obtained from a lookup table, and the resulting integers are added into a long-integer accumulator. This procedure allows the computation of the structure function within a time comparable with the time for the measurement itself.² The discrete values of Δx can be changed within steps of $0.2 \mu\text{m}$, while Δt can be changed within steps of 40 msec as given by the video frequency.

Figure 4 shows an example of a measurement of the structure function $S(\Delta x, \Delta t)$ at a subcritical value of the control parameter $\varepsilon = (V/V_c)^2 - 1 = -0.015$. A nice feature of the structure function is the fact that the noise of the camera-digitizer system piles up basically around $S(0, 0)$. There is no temporal correlation between two consecutive measurements due to the camera noise, while a spatial correlation over a couple of pixels due to the finite bandwidth of the video signal cannot be excluded. Thus, one way to obtain a noise-free measurement of the amplitude is by extrapolation to $\Delta t \rightarrow 0$. This procedure is valid only if the temporal correlation of the

² An assembly language source code for a subroutine performing the accumulation on a PC is available on request.

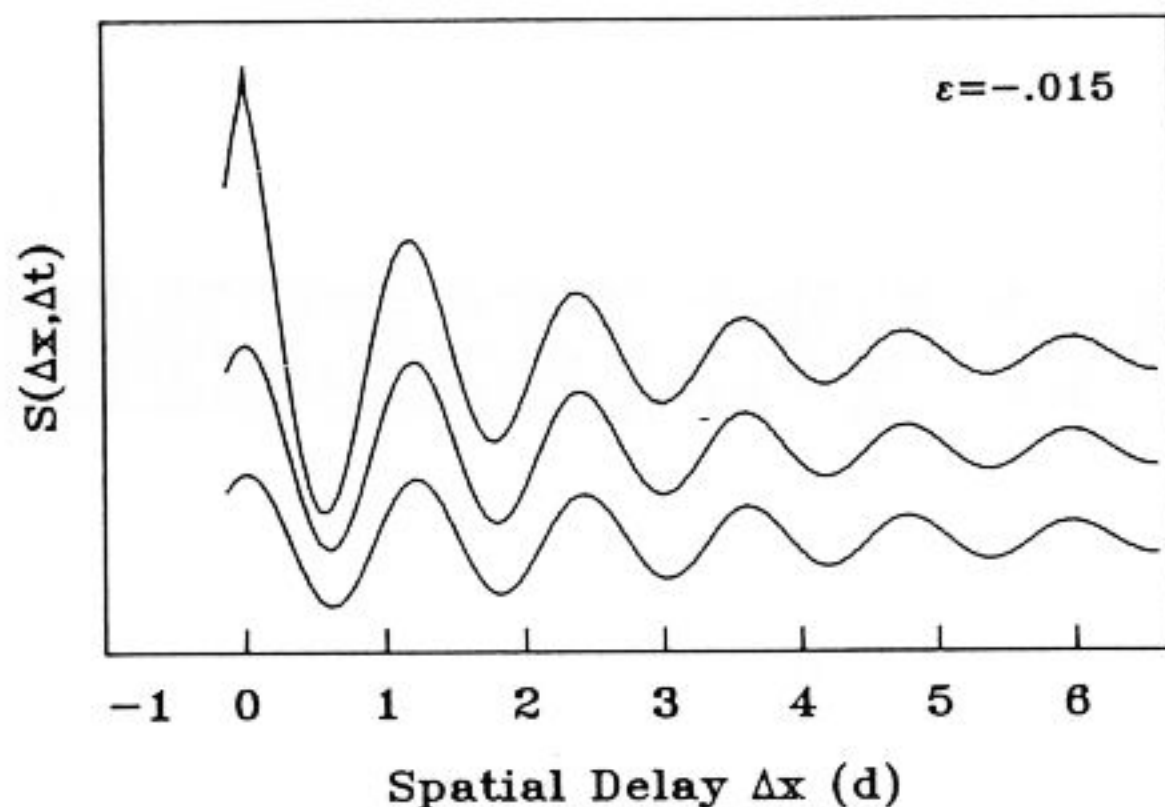


Fig. 4. The structure function $S(\Delta x, \Delta t)$ for a subcritical value of the control parameter ($\varepsilon = -0.015$). Here $\Delta t = 0$ sec for the upper curve, $\Delta t = 0.8$ sec for the middle, and $\Delta t = 1.6$ sec for the lower curve. Note the peak in the upper curve, which is primarily due to instrumental noise.

fluctuating pattern is much longer than 40 msec, however. The alternative is to ignore the values of $S(\Delta x, 0)$ for $\Delta x < 4 \mu\text{m}$ or so, which corresponds to 20 pixels of the CCD-Camera. The remaining points can then be fitted to $A^2 \cos(k \Delta x) \exp(-\Delta x/\xi)$. A combination of both methods is used in ref. 3, namely a two-dimensional fit to the theoretically expected spatiotemporal correlation function. In any case, the resulting amplitude A of the light intensity fluctuations has simply to be multiplied with the wavelength $\lambda = 2\pi/k$ and the constant 0.61 according to Eq. (1) in order to obtain the amplitude of the director fluctuations Θ .

In Fig. 5 the fluctuation amplitude obtained from these procedures for

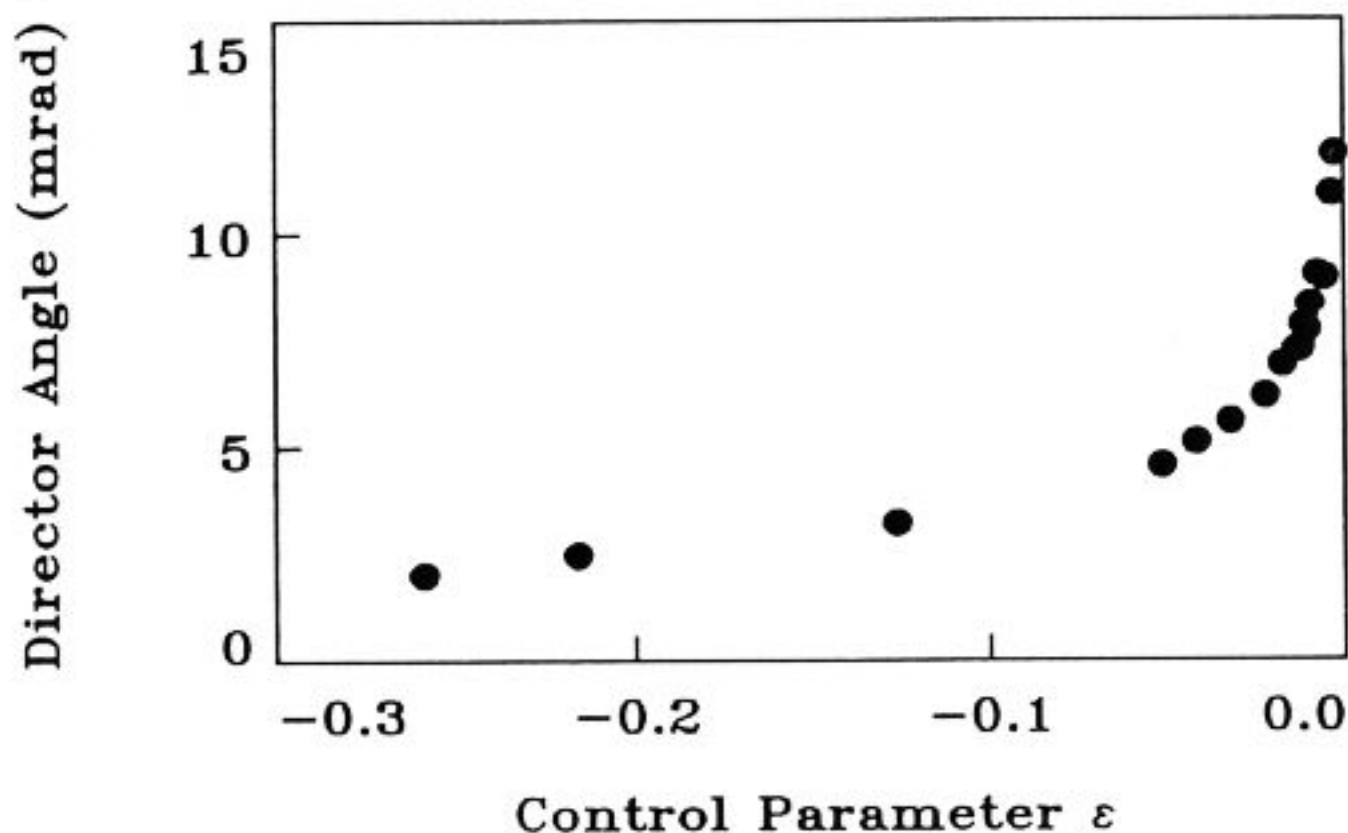


Fig. 5. The amplitude of the director fluctuations measured at subcritical values of the driving voltage.

different subcritical values of the control parameter ε is shown. It is obvious that this amplitude increases monotonically with the driving voltage. A comparison of this value with the value expected from thermodynamic fluctuations and an experimental estimation of the correlation length and correlation times of the fluctuating pattern are given in ref. 3.

In summary, the measurement method described here provides an experimental tool to detect and quantify director fluctuations of a very small amplitude even with standard equipment, where the signal-to-noise ratio is smaller than 1.

ACKNOWLEDGMENTS

We would like to thank G. Ahlers for helpful discussions. The experiments were supported by Deutsche Forschungsgemeinschaft and in part by Volkswagen-Stiftung.

REFERENCES

1. I. Rehberg, B. L. Winkler, M. de la Torre Juárez, S. Rasenat, and W. Schöpf, Pattern formation in a liquid crystal, in: *Festkörperprobleme/Advances in Solid State Physics* **29**:35–52 (1989).
2. R. Graham, Macroscopic theory of fluctuations and instabilities in optics and hydrodynamics, in: *Fluctuations, Instabilities, and Phase Transitions*, T. Riste, ed. (Plenum Press, New York, 1975).
3. I. Rehberg, S. Rasenat, M. de la Torre Juárez, W. Schöpf, F. Hörner, G. Ahlers, and H. R. Brand, Thermally induced hydrodynamic fluctuations below the onset of electroconvection, to be published.
4. S. Rasenat, G. Hartung, B. L. Winkler, and I. Rehberg, The shadowgraph method in convection experiments, *Exp. Fluids* **7**:412–420 (1989).
5. E. O. Schulz-DuBois and I. Rehberg, Structure function in lieu of correlation function, *Appl. Phys.* **24**:323–329 (1981).